Supplementary Information

Etching-Induced Electronic Modulation in Prussian Blue Analogue–Derived Metal Sulfides for Advanced Hybrid Supercapacitors

Pin-Yan Lee,[1] Kevin C.-W. Wu[1,2*] and Kuo-Chuan Ho[1,3,4**]

[1] *Department of Chemical Engineering, National Taiwan University, Taipei 10617, Taiwan*

[2] *Department of Chemical Engineering and Materials Science, Yuan Ze University, Chung-Li, Taoyuan 320315, Taiwan*

[3] *Institute of Polymer Science and Engineering, National Taiwan University, Taipei 10617, Taiwan*

[4] *Advanced Research Center for Green Mater. Science and Technology, National Taiwan University, Taipei 10617, Taiwan*

Corresponding authors:

*E-mail: kevinwu@ntu.edu.tw, Tel: +886-2-3366-3064 (Kevin W.-C. Wu)

**E-mail: kcho@ntu.edu.tw, Tel: +886-2-2366-0739 (K.C. Ho)

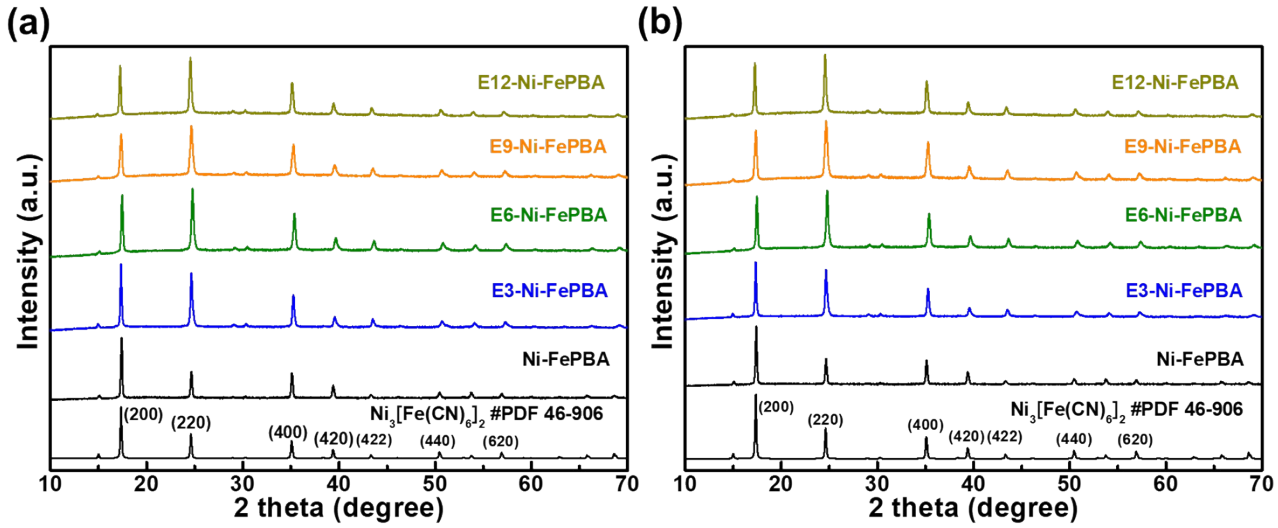

Fig. S1 XRD patterns with (a) original data and (b) normalized peak intensity at 17° of Ni-FePBA and etched Ni-FePBA.

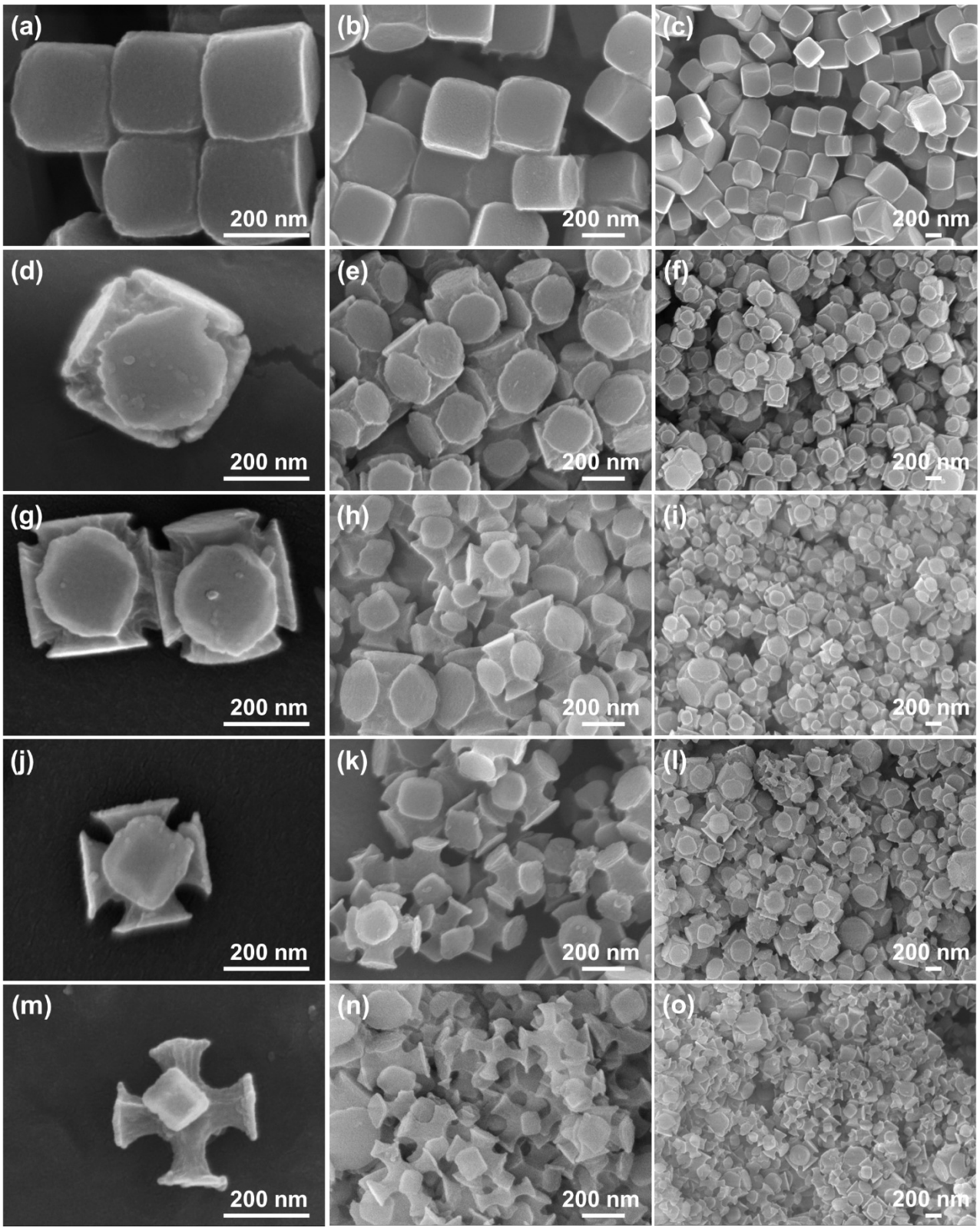

Fig. S2 SEM images of Ni-FePBA and etched Ni-FePBA. (a-c) Ni-FePBA, (d-f) E3-Ni-FePBA, (g-i) E6-Ni-FePBA, (j-l) E9-Ni-FePBA and (m-o) E12-Ni-FePBA.

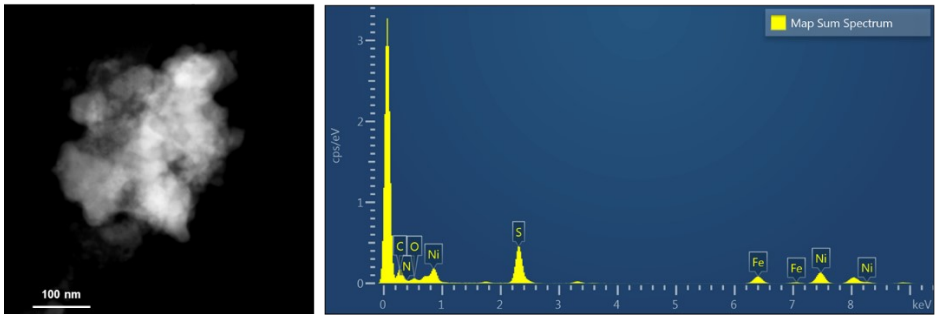

Element	Atomic %
C	57.08
N	6.16
O	6.64
S	20.73
Fe	3.66
Ni	5.74

Fig. S3 The STEM image, EDS spectrum and atomic% for elements of E9-Ni-FePBA-S.

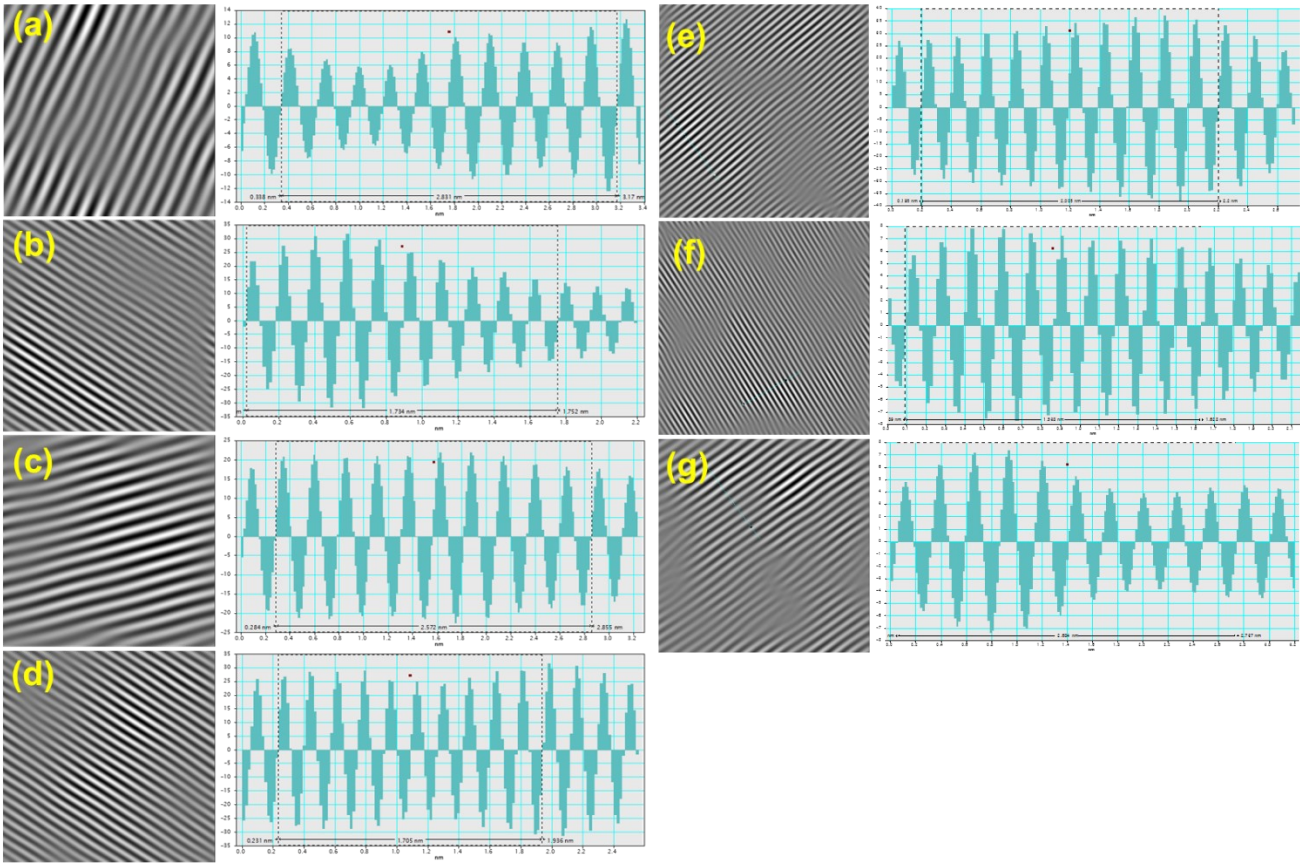

Fig. S4 HR-TEM interlayer d-spacing images of (a) NiS_2 $d_{[200]}$, (b)NiS_2 $d_{[311]}$, (c) NiS_2 $d_{[210]}$, (d) Ni_9S_8 $d_{[261]}$, (e) FeS_2 $d_{[220]}$, (f) FeS_2 $d_{[222]}$ and (g) FeS_2 $d_{[200]}$.

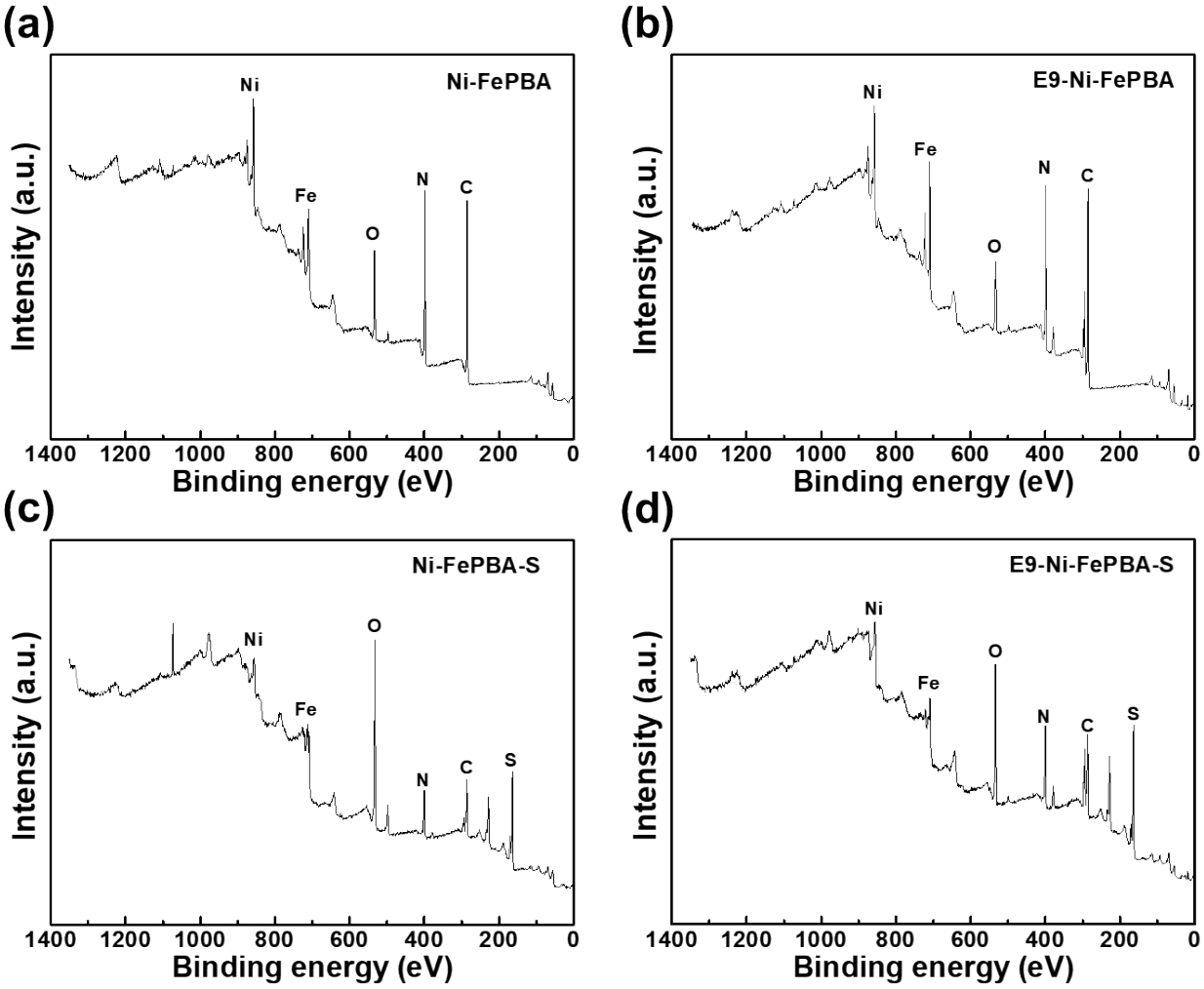

Fig. S5 XPS survey spectra of (a) Ni-FePBA, (b) E9-Ni-FePBA, (c) Ni-FePBA-S and (d) E9-Ni-FePBA-S.

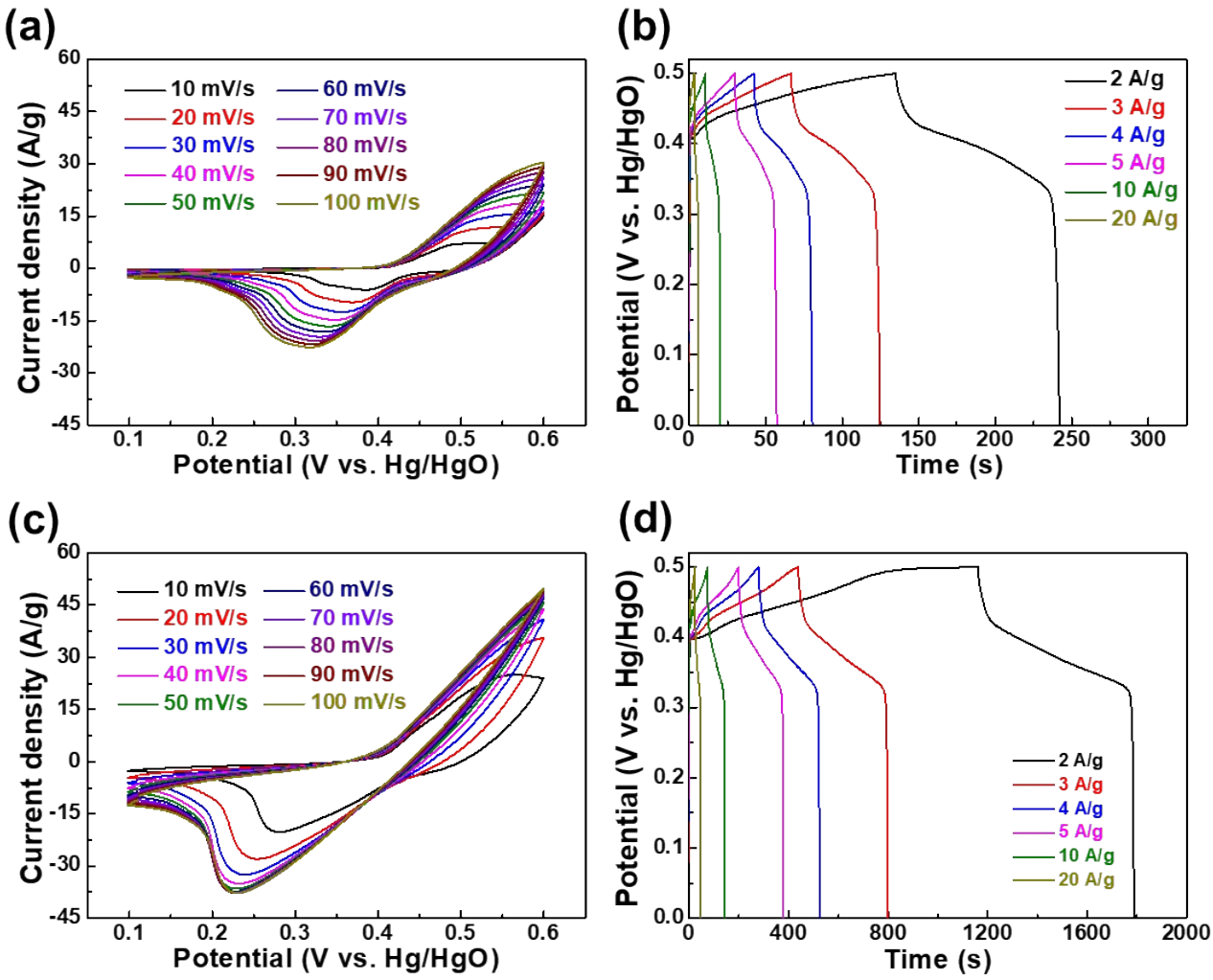

Fig. S6 (a) CV curves at different scan rates and (b) GCD profiles at different current densities of Ni-FePBA-S; (c) CV curves at different scan rates and (d) GCD profiles at different current densities of E9-Ni-FePBA-S.

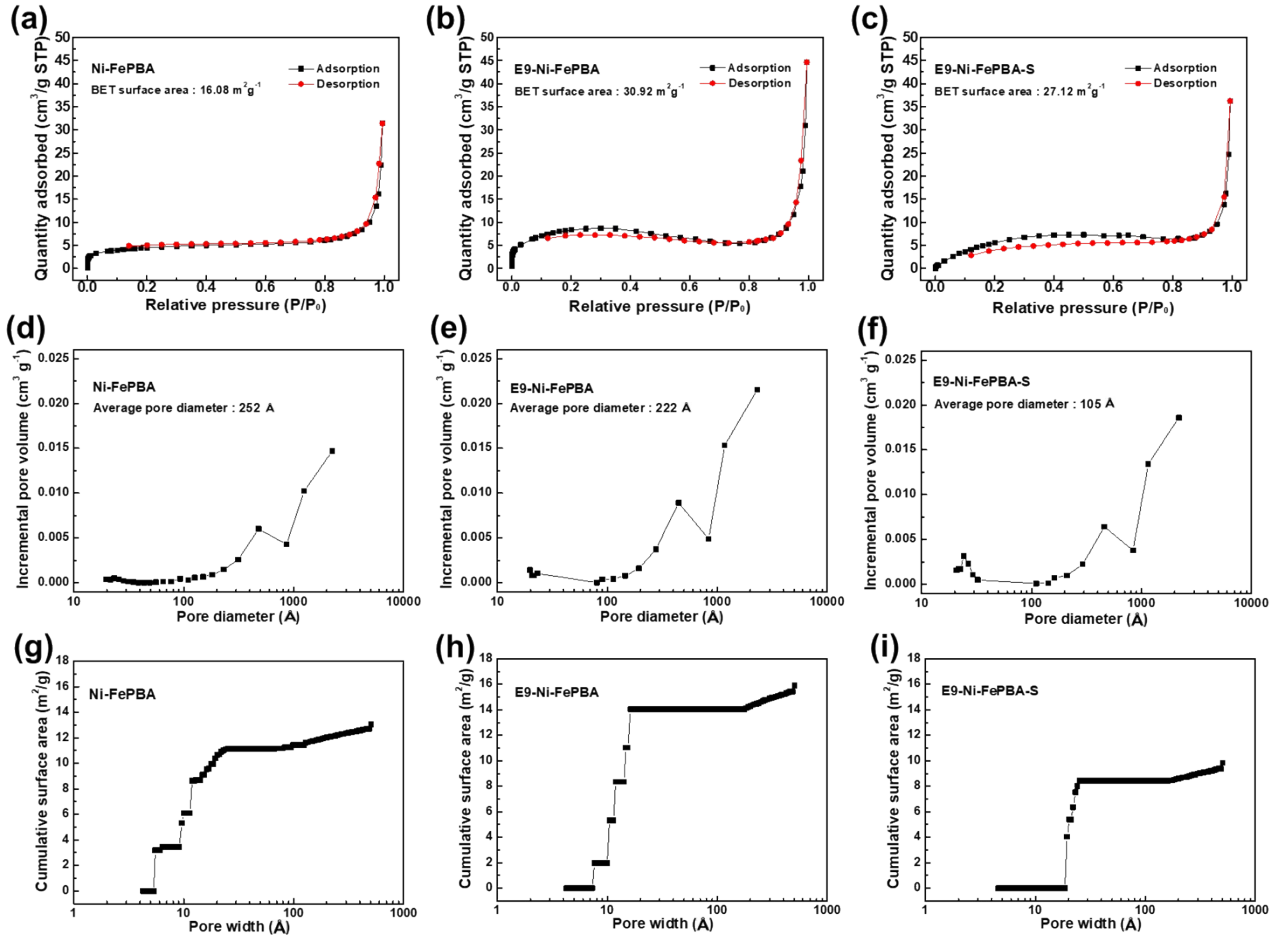

Fig. S7 The N_2 adsorption/desorption isotherms of (a) Ni-FePBA, (b) E9-Ni-FePBA and (c) E9-Ni-FePBA-S; incremental pore volume *vs.* pore diameter of (d) Ni-FePBA, (e) E9-Ni-FePBA and (f) E9-Ni-FePBA-S; cumulative surface area *vs.* pore width of (g) Ni-FePBA, (h) E9-Ni-FePBA and (i) E9-Ni-FePBA-S.

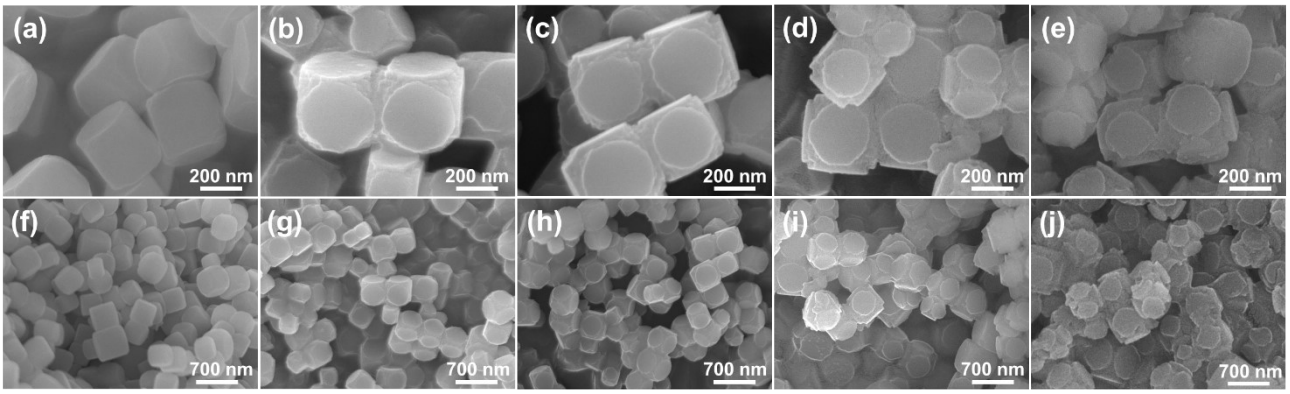

Fig. S8 The SEM images of (a, f) Ni-FePBA, (b, g) E3-NiFePBA, (c, h) E6-NiFePBA, (d, i) E9-Ni-FePBA and (e, j) E12-Ni-FePBA. The etched Ni-FePBA was synthesized with 1 M KOH and 0.66 M trisodium citrate.

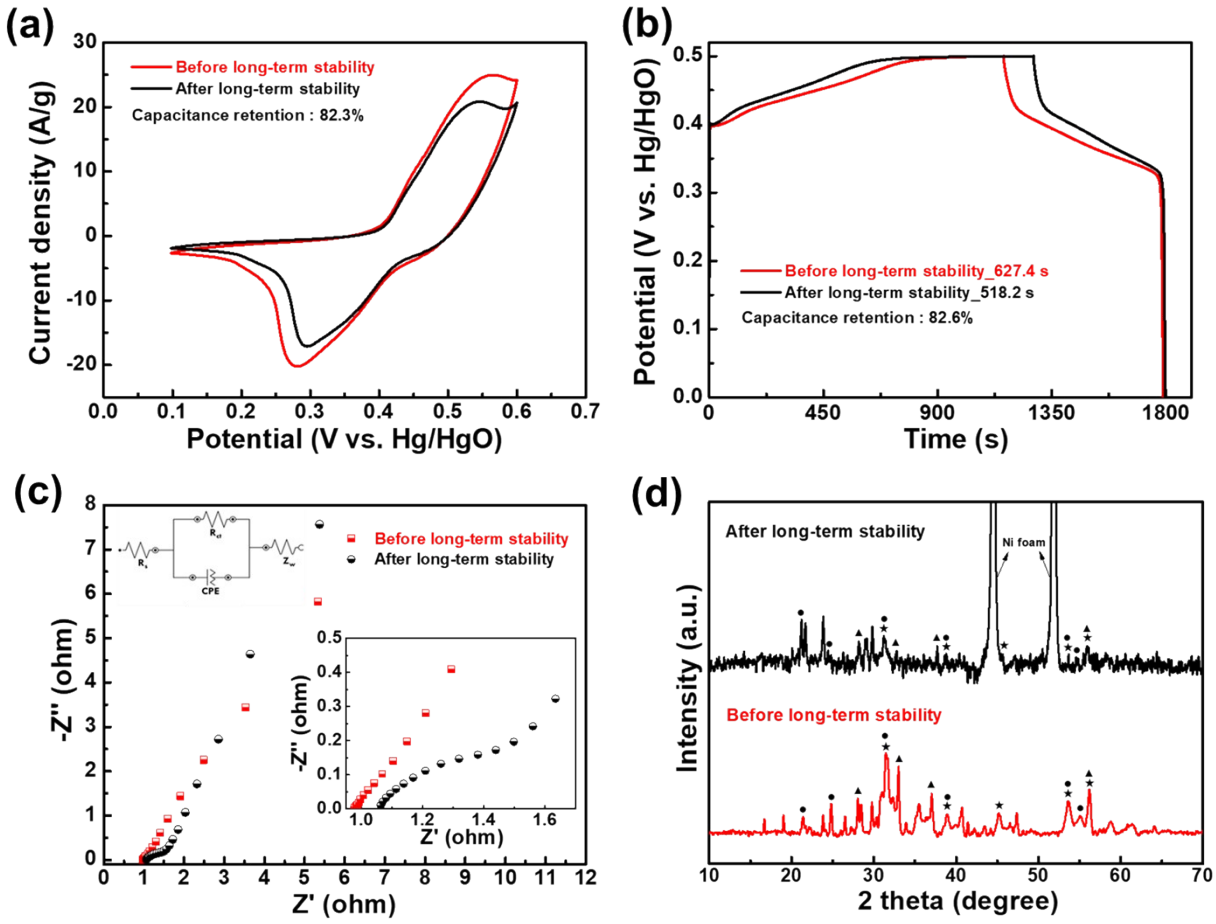

Fig. S9 The (a) CV at 10 mV/s, (b) G/CD at 2.0 A/g, (c) EIS and (d) XRD (★NiS_2 #PDF 65-3325, •Ni_9S_8 #PDF 22-1193 and ▲FeS_2#PDF 71-53) measurements for the E9-Ni-FePBA-S electrode after the long-term stability test.

Table S1. Partial lists of electrolyte and electrochemical parameters of supercapacitors based on metal sulfide materials reported in previous literature and this work.

System	Electrolyte	Potential window (V)	Specific capacitance (F/g)	Energy density (Wh/kg)	Power density (W/kg)	Ref.
Zn-doped nickel sulfide //AC	6 M KOH	1.5	6.41@1 A g^{-1}	2.14	775	[1]
NiS/NiSSe//AC	PVA/KOH	1.8	259@1 A g^{-1}	104	314	[2]
V-doped Ni_3S_2//AC	6 M KOH	1.6	123.44@1 A g^{-1}	43.89	800	[3]
Ni_3S_2@$NiMoO_4$//AC	2 M KOH	1.6	156.1@5 mA cm^{-2}	28.4	91	[4]
$Fe_5Ni_4S_8$/FeS@NHPC //AC	6 M KOH	1.5	245.8@0.5 A g^{-1}	76.8	395	[5]
Ni_3S_2@Co_3S_4//AC	6 M KOH	1.6	245@1 A g^{-1}	87.11	800	[6]
Fe-Ni-S/rGO//AC	3 M KOH	1.6	85.8@1 A g^{-1}	30.5	800	[7]
CFNSP//AC	2 M PVA/KOH	1.6	198@2 A g^{-1}	70.1	2346	[8]
Fe/NiS_2//AC	2 M KOH	1.6	132.67@1 A g^{-1}	-	-	[9]
Fe-Co-S//AC	2 M KOH	1.6	168.6@1 A g^{-1}	65.9	803	[10]
Ni_3S_2-Co/Fe-5//AC	6 M KOH	1.5	212@1 A g^{-1}	66.25	748	[11]
E9-Ni-FePBA-S//AC	2 M KOH	1.6	88.38@2 A g^{-1}	31.4	1600	This work

References

1. Moradi, M., S. Zolfaghari, M. Pooriraj, M. Babamoradi, and S. Hajati, One-step synthesis of Zn-doped nickel sulfide/graphene derived from Ni-MOF for supercapacitor application, Materials Chemistry and Physics, 329 (2025) 130068.
2. Caroline, S.C., B. Das, S.S. Pramana, and S.K. Batabyal, Nickel sulfide-nickel sulfoselenide nanosheets as a potential electrode material for high performance supercapacitor with extended shelf life, Journal of Energy Storage, 68 (2023) 107812.
3. Yan, C., X. Yang, S. Lu, E. Han, G. Chen, Z. Zhang, H. Zhang, and Y. He, Hydrothermal synthesis of vanadium doped nickel sulfide nanoflower for high-performance supercapacitor, Journal of Alloys and Compounds, 928 (2022) 167189.
4. Xie, Z., D. Dai, Y. Xue, Y. Li, L. Liu, D. Yu, L. Han, Y. Hua, X. Zhao, and X. Liu, Synthesis of hierarchical Ni_3S_2@$NiMoO_4$ core-shell nanosheet arrays on Ni foam for high-performance asymmetric supercapacitors, Journal of Energy Storage, 44 (2021) 103459.
5. Sun, H., L. Zheng, Y. Xi, S. Zhai, Q. An, and Z. Xiao, Nickel-iron sulfide nanoparticles

supported on biomass-derived N-doped hierarchical porous carbon as a robust electrode for supercapacitors, Electrochimica Acta, 466 (2023) 143053.
6. Wang, X., F. Zhou, R. Jing, S. Gu, Q. Zhang, Z. Li, Y. Zhu, Z. Xiao, and L. Wang, The precise building units modulation of iron-bismuth sulfide triple-level hierarchical structure for enhanced supercapacitor performance, Journal of Power Sources, 597 (2024) 234128.
7. Zeng, X., M. Yang, J. Zhao, J.-J. Shao, and Z. Ding, Iron-doped nickel sulfide nanospheres anchored on reduced graphene oxide for high performance supercapacitors, Materials Chemistry Frontiers, 8 (2024) 1816-1826.
8. Premkumar, M. and S. Vadivel, Fabrication of binder-free CNT/$FeNiS_2$@PPy mixed metal sulfide loaded Ni Foam as cathode material for asymmetric supercapacitor applications, Journal of Energy Storage, 69 (2023) 107948.
9. Wang, H., M. Liang, and Z. Miao, Engineering accordion-like Fe-doped NiS_2 enabling high-performance aqueous supercapacitors and Zn-Ni batteries, Chemical Engineering Journal, 470 (2023) 144148.
10. Zhao, J., H. Yang, S. Dong, Y. Wang, X. Lv, Q. Zhang, and L. Wen, Fe-Co-S nanoarrays on nickel foam as binder-free electrodes for energy storage and electrocatalysis, Chemical Engineering Journal, 494 (2024) 152808.
11. Yang, F., L. Zhang, Z. Zhang, and W. Dong, Facile synthesis of Co/Fe bimetallic doped Ni_3S_2 nanosheets and supercapacitor performance, Journal of Energy Storage, 104 (2024) 114568.